Research Article

Piezoelectric Property from Processed Prawn Shells

Ramar Marimuthu*, Sabarmathi Ravichandran, Aarthi Suresh

College of Fisheries Engineering, Tamil Nadu Dr. J. Jayalalithaa Fisheries University, Nagapattinam - 611 002, Tamil Nadu, India

Abstract

The piezo-electric film was developed from bio-waste of Prawn Shells (PS). The absorption peak of PS film was observed at 266 nm and 377 nm, respectively. The PS is about 40% - 46% transmittance in the spectral visible region. The PS film contains 20% - 40% protein, 20% - 50%, calcium carbonate, and 15% - 40% chitin, after demineralization, only chitin nanofibers (ChNFs) act as an active piezoelectric element. The co-existence of intra and inter-molecular hydrogen bonds is also evident from the vibrational bands of 3145cm^{-1} and 3011cm^{-1}, respectively. The X-ray diffraction analysis two diffraction peaks are observed at 2θ ~ 19.82º and 39.56º, respectively. The cross-sectional image of PS shows hierarchically organized and specially arranged layer structure of ChNFs. The flexibility of processed prawn shell film will be used as energy harvesting device applications.

Keywords: bio waste, prawn shell, piezo-electric, demineralization, energy harvesting

***Correspondence**

Author: Ramar Marimuthu

Email: ramar@tnfu.ac.in

Introduction

Piezoelectric materials are a group of substances that show electric replications (e.g., the accumulation of charges on the surface) when subject to mechanical stress. The early piezoelectric material-Rochelle salt was first synthesized for medical purposes in the tardy 17th century [1, 2]. It was the Curie brothers who first discovered the piezoelectric effect as they demonstrated that the effect is proximately associated with crystal structures by directly optically canvassing the piezoelectric behaviors from solids like quartz, cane sugar, Rochelle salt etc [3]. By looking into the crystallography, 20 crystal classes were found to exhibit the direct piezoelectric effect due to the lack of central symmetry in the unit cell, leading to the emergence of perovskite barium titanate (BTO) and the lead zirconate titanate (PZT) family around the world war II [4, 5]. Another milestone in the evolution of piezoelectric materials is the revelation of decent piezoelectric coefficients (20–30 pC/N for d_{33} and 16 pC/N for d_{31}) from synthetic polymers, such as polyvinylidene fluoride (PVDF) [6, 7]. Nowadays, incipient inorganic and organic piezoelectric materials with advanced properties and broader functionalities are perpetually being discovered and engendered [8, 9].

Piezoelectrics are essential in the modern society. Their applications cover extensive fields from automobiles (e.g., tire monitoring [10], fuel injector [11]) to architectures (e.g., building and bridge oscillation monitoring [12]), from biomedicals (e.g., ultrasonic imaging [13], wireless pacemaker [14] and implantable energy harvester [15]) to daily necessaries (e.g., shoes [15], verbalizers [16] and transformers [17]), and from advanced instruments (e.g., inkjet printer [18], atomic force microscope [19]) to militaries (e.g., robotics [20]). On the other hand, the raising vigilance of lead leaching from the best-performed PZT family is undermining its application potential [21]. Alternative lead-free piezoceramics (BTO and potassium sodium niobate (KNN) predicated materials) are facing challenges from recycling of their waste while destitute of flexibility [22]. The degradation of PVDF could engender toxic HF that is detrimental to both environment and humanity [23].

As bioelectronics typically interface human bodies, conventional piezoelectric materials have great concerns of biosafety and biocompatibility. In addition, biodegradability, the capability for biological degradation of organic materials by living organisms down to the base substances, is another greatly desired feature, which can circumvent additional surgical procedures and introduce superb biocompatibility and environmental conviviality [24, 25]. Consequently, novel piezoelectric materials with ideal biodegradability are the trend for the incipient generation of implantable and wearable bioelectronics.

Environmental pollution is a natural consequence of human activities. It is also the result of natural processes. In the course of human development, industrialization has made possible higher standards of living in our modern society. Such "progress" has engendered incremented quandaries with wastes from processing operations and their ultimate disposal engendering dihydrogen monoxide pollution, air pollution and land pollution [26].

The nature of waste is wide and varied, being broadly relegated into: agricultural, municipal and industrial. The latter source inclines to engender waste of the most polluting types, the majority being chemicals (37.6% of the total) and metals (29.1%). The remnant of the industrial wastes includes such diverse materials as paper (4.6%), petroleum (2.4%), stone, rubber, leather and textiles. Of this wide range of industrial waste, some 3% is engendered by the aliment processing industries [27]. Such waste is, however, amenable to forms of treatment because of its organic nature. Organic food waste contains proteins, vitamins, carbohydrates, fat and such components are highly polluting due to what is termed their high Biochemical Oxygen Demand (BOD). They are also, however, astronomically valuable components which can be recuperated.

The shell fish industry is operative among all the costal countries and contributes hugely to the victuals delicacies. During the processing of prawns, shrimps and lobsters mostly the meat is taken, while the shell and head portions are engendered as wastes. This results in the generation of a plethora of waste throughout the world. It is estimated that the shell-fish industry engenders about 60,000-80,000 tons of waste. The disposal of such a huge amount of waste has become an earnest environmental concern [28]. Albeit these wastes are biodegradable but the rate of degradation of a huge amount of waste engendered per processing operation is comparatively slow [29]. This results in accumulation over time and the ads to environmental concerns as they not only engender obnoxious smell but also magnetize pathogenic insects, flies and rodents, thus engendering an unhygienic atmosphere. The immediate solution to this quandary seems to be expeditious recycling of the crustacean shells engendered and extraction of commercially viable substances to be further utilized in other applications [30].

In this paper, we have developed piezo-electric film from bio-waste of PS and the most recent major advancements in biodegradable piezoelectric materials. We first introduce The UV-visible spectroscopy and spectrophotometer studies have been characterized at the molecular level. The Energy dispersive x-ray analysis (EDAX), Fourier transform infrared (FT-IR) spectroscopy, X-ray diffraction (XRD) pattern, Raman spectroscopy and scanning electron microscopy (SEM) characteristics have been studied. The main objective of this paper focuses on novel piezoelectric biomaterials sharing the unique characteristic of biodegradability, providing insights into their origin of piezoelectricity, as well as new application opportunities as wearable and implantable bioelectronics.

Experiment

Bio-waste of raw prawn shells were collected from the nearby seafood processing plant (**Figure 1a**). In particular, prawn shells selected for this work to make transparent suitable flexible substrate for the applications of energy harvesting devices. Then, prawn shells were washed thoroughly with deionized water followed by demineralization process. A solvent system was prepared by mixing of NaOH pellet (Merk) with deionized water and then 1.0 M NaCl (Merk), 0.05 M Tris HCl (Merk), 20.0 mM EDTA (Merk) were mixed together to wash the shells. Finally, the transparent and flexible demineralised prawn shells were achieved by stirring the shells in a solution of 0.5 M EDTA. The average thickness of used prawn shell was 130±10 μm. The UV-visible spectroscopy and spectrophotometer, Energy dispersive x-ray analysis (EDAX), Fourier transform infrared (FT-IR) spectroscopy, X-ray diffraction (XRD) pattern, Raman spectroscopy and scanning electron microscopy (SEM) characteristics have been studied. The prawn shells which is not only transparent (~ 60% to 40% transparency) but also rollable that makes suitable flexible substrate for wearable and implantable bioelectronics.

Results and Discussion

Figure 1 shows that digital photograph of bio waste of prawn shells, washed and processed prawn shells. The absorption spectrum of PS was studied by UV-Vis absorption spectroscopy as shown in **Figure 2**. The maximum absorption was observed at a wavelength of 266 nm and 377 nm, respectively. This peaks are indicates confirm of piezoelectric material property of the prawn shell.

The transmission spectrum of PS was characterized by spectrophotometer as shown in **Figure 3**. The PS is about 40 % - 46 % transmittance in the spectral visible region of 400 - 900 nm. The transmissions values are compared to the already reported values are virtually same. Because of the substantiation value, the developed PS film has piezoelectric property. The prawn shell was exhaustively washed with deionized dihydrogen monoxide followed by a simple demineralization process to abstract the unwanted minerals. The PS film contains 20 % - 40 % protein, 20 % - 50 % calcium carbonate, and 15 % - 40 % chitin, after demineralization, only chitin nanofibers (ChNFs) act as an active piezoelectric element [31]. The minerals study was done by energy dispersive x-ray analysis (EDAX) as shown in **Figure 4**. Deminaralized prawn shells are analyzed using energy dispersive x-ray analysis for finding the element composition in it. Energy dispersive x-ray analysis helps us find the mineral components and its combinations in the prawn shells that can be used for further research work.

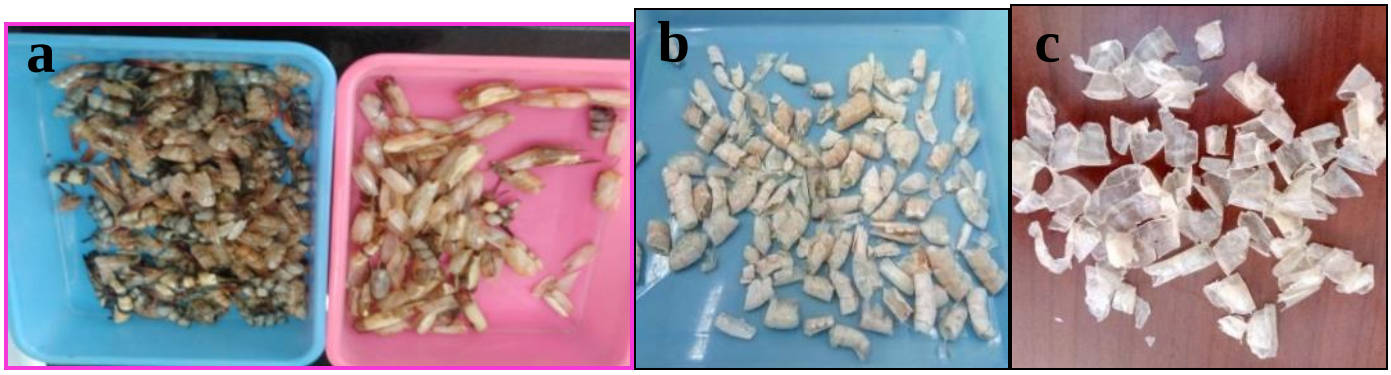

Figure 1 (a) Bio waste of prawn shells, (b) Washed prawn shells and (c) Processed prawn shells

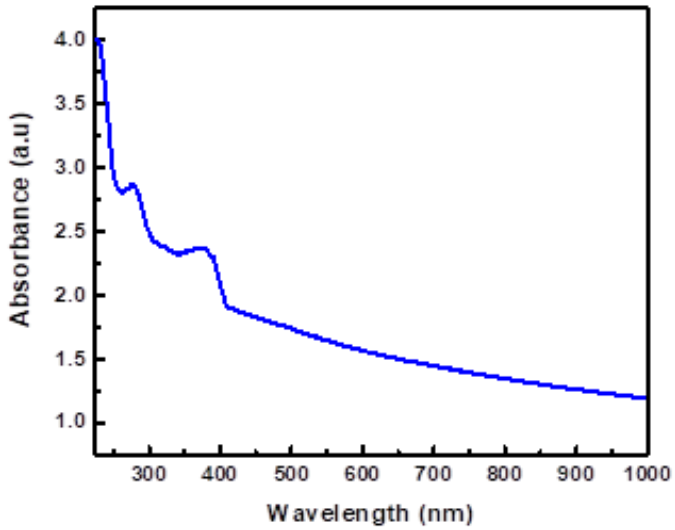

Figure 2 UV-Absorption spectra of the Prawn Shell

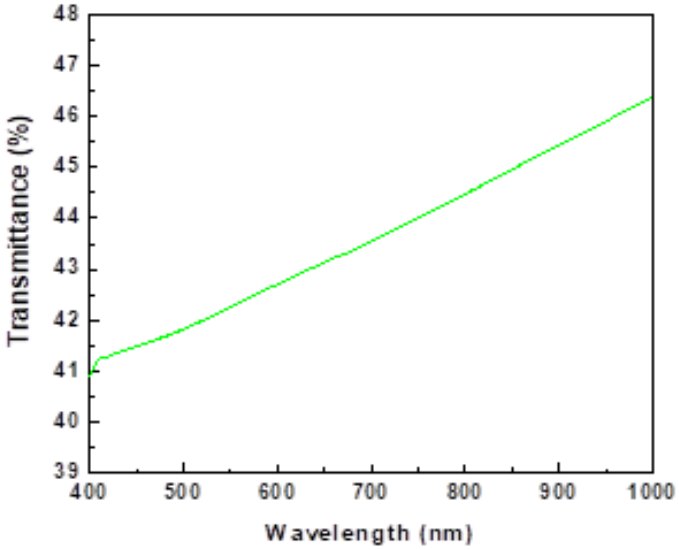

Figure 3 Transmission characteristics of the Prawn Shell

The structural and crystallographic features of PS were studied by FT-IR spectroscopy (**Figure 5**). The co-existence of intra and inter-molecular hydrogen bond is also conspicuous from the vibrational bands of 3145 cm^{-1} and 3011 cm^{-1}, respectively, as shown in Figure 5. In integration, the splitting of amide I peak into two peaks unequivocally denotes the engagement of intra-molecular hydrogen bonds (1620 cm^{-1}) along with the inter-sheet C=O…NH hydrogen bonds (1650 cm^{-1}). Furthermore, the absorption band at 1548 cm^{-1} manifests the presence of amide II band [32]. Thus, α-chitin consisting of a vigorous hydrogen bonding network structure belongs to the chiral space group $P2_12_12_1$, sanctioning macroscopic polarization in the fiber through the axial vector properties [32-34].

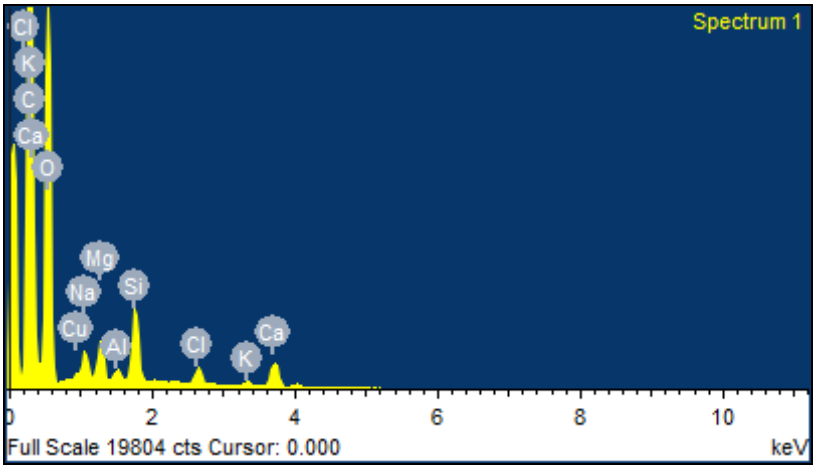

Figure 4 Mineral composition of demineralized prawn shell

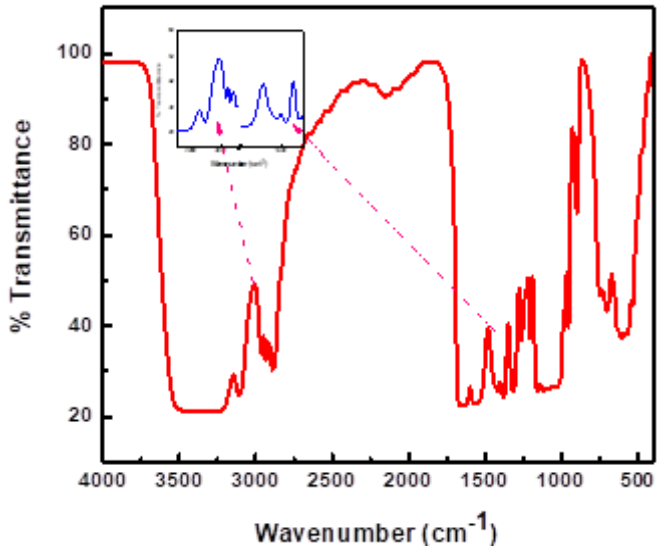

Figure 5 FTIR Spectra of the Prawn Shell (Inside figure shows the maximized peak)

In the X-ray diffraction (XRD) pattern, three diffraction peaks are optically canvassed at 2θ ~ 9.96°, 19.82º and 24.05º, respectively in the range of 15º - 30º as shown in **Figure 6**. Noteworthy, two main diffraction peaks arising from the inter-sheet (2θ~9.96°) and intra-sheet (2θ~19.82°) crystallographic planes are the characteristics of α-chitin [35]. The anti-parallel molecular arrangement of α-chitin sanctions the inter-sheet hydrogen bonds to occur with the intra-sheet hydrogen bonds at the same time [32].

The presence of amino acids in the triple helix structure of the polypeptide chains is confirmed by Raman spectroscopy (**Figure 7**). For example, the band arises at 1671 cm^{-1} due to stretching (ν) vibration of carbonyl group (ν (C=O)) of peptide backbone in Gly-X-Y tripeptide sequence, attributed to amide I band. The strong absorbance at 1456 cm^{-1} corresponds to the CH_2 deformation (d (CH_2)). The vibrational bands arise at 1279 cm^{-1} and 1250 cm^{-1} due to in plane deformation of N-H (δ (N-H)) coupled to C-N stretching mode (ν (C-N)), respectively, ascribed to amide III band. This band signifies the polar triple helix structure of collagen. Additionally, bands corresponding to carboxyl groups (such as at 1432 cm^{-1} from aspartic acid and 1060 cm^{-1} from glutamic acid) and protonated amino residues, i.e., NH_3 (1110 cm^{-1}), are also observed. The region of 1000-800 cm^{-1} in the spectra is very much significant where amino acids such as Phenylalanine (1037 and 1007 cm^{-1}), Proline (Pro) (917 and 855 cm^{-1}), and Hydroxyproline (Hyp) (881 cm^{-1}) show strong Raman scattering due to aromatic or saturated side chain rings. The peak at 942 cm^{-1} represents the C-C stretching (ν CC)) vibration of the peptide backbone. Thus, Raman spectrum confirms the presence of helical structure in collagen of prawn shells with the tripeptide sequence of Gly-Pro-Y and Gly-X-Hyp.

The cross-sectional scanning electron microscopy (SEM) image of the prawn shell shows hierarchically organized and specially arranged layer structure of chitin nanofiber (ChNFs) (**Figure 8**). Those are oriented horizontally in-plane parallel to the smooth surface. The average diameter of the ChNFs is 25 nm. The detailed surface morphologies were investigated by SEM operated at an acceleration voltage of 20 kV.

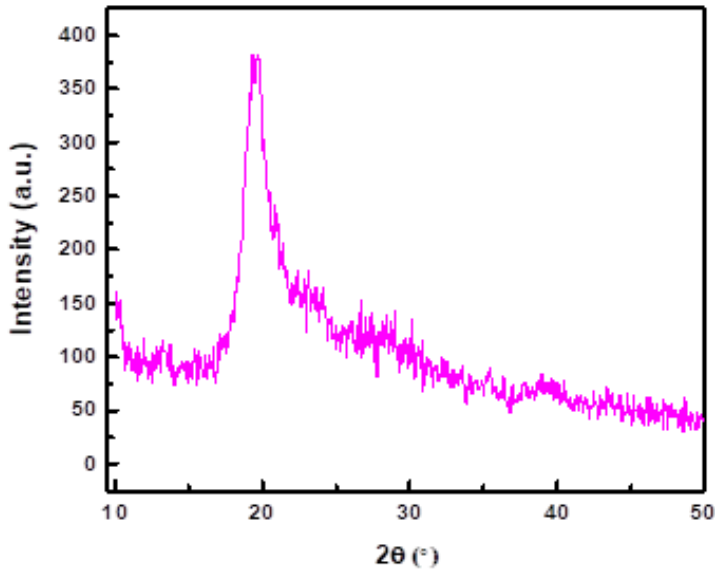

Figure 6 XRD pattern of prawn shell

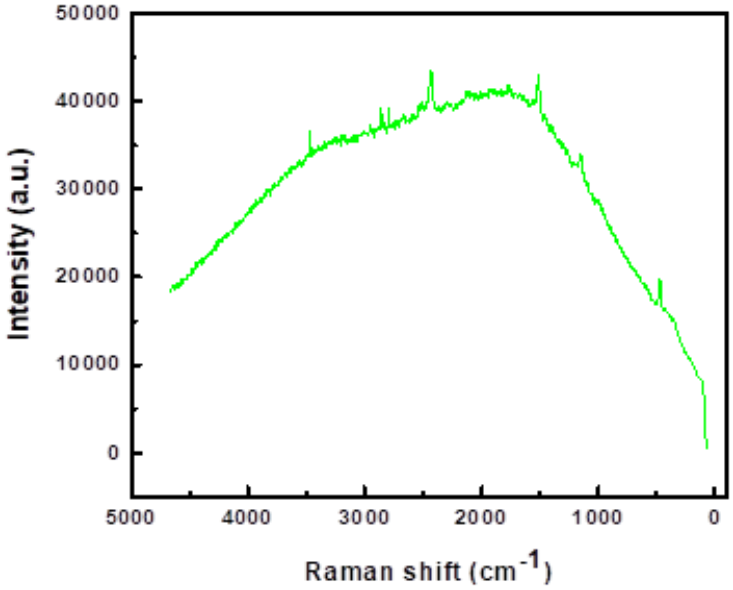

Figure 7 Raman spectra of the prawn shell

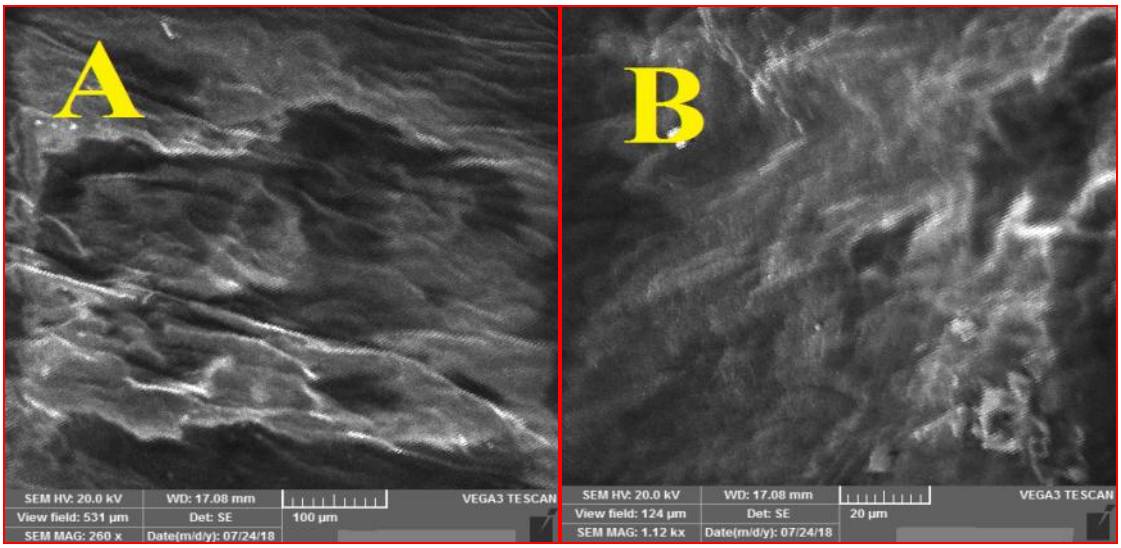

Figure 8 Scanning electron microscopy (SEM) image of the prawn shell

Figure 9 (a) and (b) shows that the transparency of the prawn shell and flexibility of the prawn shell at 360°. The flexibility of prawn shell film will be used as energy harvesting devices of nano-generator and sensor applications. The energy output voltages vary with applied pressure change as shown in **Figure 10**. The different output voltages are measured at 23.2 mV, 44.9 mV, 57.8 mV and 88.5 mV varies with applied pressure change. The changing of applied pressure of disc output voltages also changed depends upon the pressure value. When we apply a lesser amount of pressure, only small amount of output voltages are produced. To produce huge amount of energy output, the experimental setup can be connected in series connection mode.

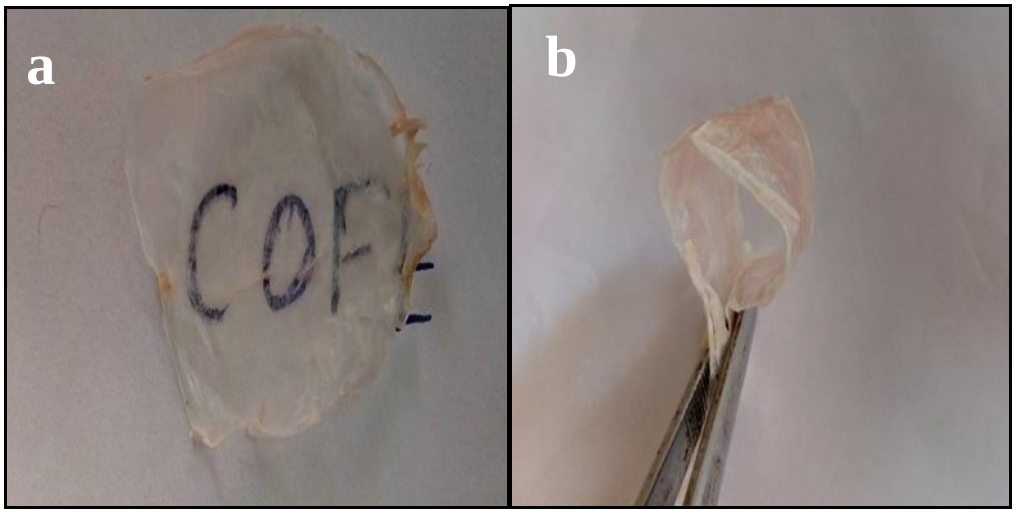

Figure 9 (a) Transparency of the prawn shell and (b) Flexibility of the prawn shell at 360°

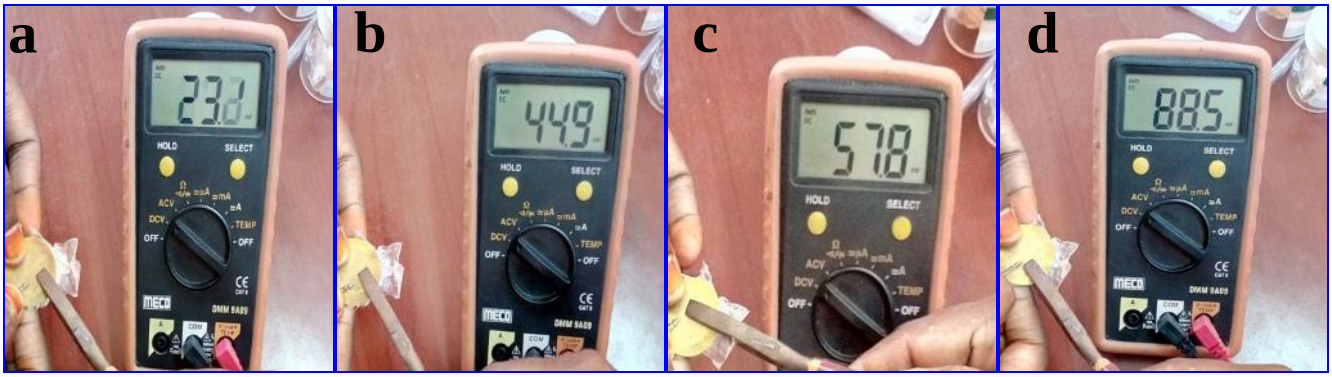

Figure 10 The different output voltage of (a) 23.2 mV, (b) 44.9 mV, (c) 57.8 mV and (d) 88.5 mV varies with applied pressure intensity

Conclusion

The piezo-electric film has been studied from PS. The absorption peak of the PS film has been observed at 266 nm and 377 nm, respectively. The transmittance of PS was confirmed in the spectral visible region of 400 - 900 nm. Fourier transform infrared (FT-IR) spectroscopy was studied by structural and crystallographic features. The X-ray diffraction (XRD) pattern, Raman spectroscopy and cross-sectional scanning electron microscopy (SEM) image confirm the piezo-electric properties. The flexibility prawn shell films of energy output voltages vary with applied pressure change have been studied.

Acknowledgement

The first author gratefully acknowledge the Tamil Nadu Dr. J. Jayalalithaa Fisheries University for funding of University Research Project (URP No. 06/DR/TNFU/2017).

References

[1] G. Busch, Early history of ferroelectricity, Ferroelectrics, 1987, 74:267-284
[2] J. Valasek, Piezo-electric and allied phenomena in Rochelle salt, Physical Review, 1921, 17:475-481.

[3] W. P. Mason, Piezoelectricity, Its history and applications, The Journal of the Acoustical Society of America, 1981, 70:1561-1566.
[4] G. H. Haertling, Ferroelectric Ceramics: History and Technology, Journal of American Ceramic Society, 1999, 82:797-818.
[5] M. Acosta, N. Novak, V. Rojas, S. Patel, R. Vaish, J. Koruza, G. Rossetti, Jr, J. Rodel, BaTiO3-based piezoelectrics: Fundamentals, current status, and perspectives, Applied Physics Reviews, 2017, 4:041305-1-53.
[6] R. Kepler, Ferroelectricity in polyvinylidene fluoride, Journal of Applied Physics, 1978, 49:1232-1235.
[7] H. Kawai, The Piezoelectricity of Poly (vinylidene Fluoride), Japanese Journal of Applied Physics, 1969, 8:975-976.
[8] W.Q. Liao, D. Zhao, Y.Y. Tang, Y. Zhang, P.F. Li, P.P. Shi, X.G. Chen, Y.M. You, R.G. Xiong, A molecular perovskite solid solution with piezoelectricity stronger than lead zirconate titanate, Science, 2019, 363:1206-1210.
[9] H.Y. Zhang, Y.Y. Tang, P.P. Shi, R.G. Xiong, Toward the Targeted Design of Molecular Ferroelectrics: Modifying Molecular Symmetries and Homochirality, Accounts of Chemical Research, 2019, 52:(7)1928-1938.
[10] Z. Yang, S. Zhou, J. Zu, D. Inman, High-performance piezoelectric energy harvesters and their applications, Joule, 2018, 2:642-697.
[11] M. Senousy, F. X. Li, D. Mumford, M. Gadala, R. K. N. D. Rajapakse, Thermo-electro-mechanical performance of piezoelectric stack actuators for fuel injector applications, Journal of Intelligent Material Systems And Structures, 2009, 20:387-399.
[12] M. Iqbal, F.U. Khan, Hybrid vibration and wind energy harvesting using combined piezoelectric and electromagnetic conversion for bridge health monitoring applications, Energy Conversion and Management, 2018, 172:611-618.
[13] Q. Zhou, K.H. Lam, H. Zheng, W. Qiu, K.K. Shung, Piezoelectric single crystal ultrasonic transducers for biomedical applications, Progress in Materials Science, 2014, 66:87-111.
[14] N. Li, Z. Yi, Y. Ma, F. Xie, Y. Huang, Y. Tian, X. Dong, Y. Liu, X. Shao, Y. Li, Direct Powering a Real Cardiac Pacemaker by Natural Energy of a Heartbeat, ACS Nano, 2019, 13:(3) 2822-2830.
[15] J. Li, X. Wang, Research Update: Materials design of implantable nanogenerators for biomechanical energy harvesting, APL Materials, 2017, 5:(073801)1-15.
[16] S.C. Ko, Y.C. Kim, S.S. Lee, S.H. Choi, S.R. Kim, Micromachined piezoelectric membrane acoustic device, Sensors and Actuators A: Physical, 2003, 103:130-134.
[17] J. Yang, Piezoelectric transformer structural modeling - A review, IEEE Transactions on ultrasonics, ferroelectrics, and frequency control, 2007, 54(6):1154-1170.
[18] R. E. Saunders, J. E. Gough, B. Derby, Delivery of human fibroblast cells by piezoelectric drop-on-demand inkjet printing, Biomaterials, 2008, 29:193-203.
[19] G. Binnig, C. F. Quate, C. Gerber, Atomic force microscope, Physical Review Letters. 1986, 56:(9) 930-933.
[20] Y. Wu, J. K. Yim, J. Liang, Z. Shao, M. Qi, J. Zhong, Z. Luo, X. Yan, M. Zhang, X. Wang, Insect-scale fast moving and ultrarobust soft robot, Science Robotics, 2019, 4:eaax1594 (1-9).
[21] J. Rodel, K. G. Webber, R. Dittmer, W. Jo, M. Kimura, D. Damjanovic, Transferring lead-free piezoelectric ceramics into application, Journal of the European Ceramic Society, 2015, 35:1659-1681.
[22] K. Okada, T. Yanagisawa, Y. Kameshima, A. Nakajima, Properties of TiO_2 prepared by acid treatment of $BaTiO_3$, Materials Research Bulletin, 2007, 42:19211929
[23] F. Liu, N. A. Hashim, Y. Liu, M.M. Abed, K. Li, Progress in the production and modification of PVDF membranes, Journal of Membrane Science, 2011, 375:1-27.
[24] M. J. Tan, C. Owh, P. L. Chee, A. K. K. Kyaw, D. Kai, X. J. Loh, Biodegradable electronics: cornerstone for sustainable electronics and transient applications, Journal of Materials Chemistry C, 2016, 4:5531-5558.
[25] V. R. Feig, H. Tran, Z. Bao, Biodegradable polymeric materials in degradable electronic devices, ACS Central Science, 2018, 4(3)337-348.
[26] C. J. Brine, P. A. Sandford, J. P. Zikakis, Advances in chitin and chitosan, Science Publishers, London Elsevier, 1992, 404.
[27] W.F. Stevens, M.S. Rao, S. Chandrkrachang, Chitin and chitosan-environmental friendly and versatile biomaterials. The proceedings of the second Asia Pacific Symposium, 1996, Bioprocess Technology Program, Asian Institute of Technology, Bangkok, Thailand.
[28] R. Muzzarelli, C. Jeuniaux, G.W. Gooday, Chitin in nature and technology, Plenum Publishing Corporation, New York, 1986.
[29] R. Prashanth, R. Tharanathan, Chitin/chitosan: modifications and their unlimited application potential- an

overview, Trends in Food Science & Technology, 2007, 18:117-131.
[30] G. A. F. Roberts, Thirty Years of Progress in Chitin and Chitosan, Progress on chemistry and application of chitin and its, 2008, 8:7- 15.
[31] N. Yan and X. Chen, Don't waste seafood waste, Nature, Nature, 2015, 524:155-1575.
[32] M. Rinaudo, Chitin and chitosan: Properties and applications, Progress in Polymer Science, 2006, 31:603-632.
[33] E. Fukada and S. Sasaki, Dynamic mechanical behavior of chitin and chitosan, Journal of Polymer Science Polymer Physics Edition, 1975, 13:1845.
[34] T. Putzeys and M. Weubbenhorst, IEEE transactions on dielectrics and electrical insulation, 2015, 22:1394.
[35] J. Jin, D. Lee, H. G. Im, Y. C. Han, E. G. Jeong, M. Rolandi, K. C. Choi, and B. S. Bae, Chitin Nanofiber Transparent Paper for Flexible Green Electronics, Advanced Materials, 2016, 28:1-7.

Publication History
Received 10.09.2020
Revised 07.10.2020
Accepted 29.10.2020
Online 30.11.2020